Schematic plans of typical tetrahedra used for calibration are shown in figure 2. The electrical resistance between the two contact tabs labelled T depends upon the resistances of bismuth and thallium components, and these increase with increasing pressure at constant temperature. The bismuth I → III, bismuth II → III and thallium II → III transitions show up as slope discontinuities in the measured resistance. As the resistance of the bismuth and thallium is small, measurements are made with an AC Kelvin double bridge. The off-balance potential of the bridge is detected and continuously monitored using an amplifier and phase-sensitive detection system. Changes of the order of $10^{-6}\,\Omega$ can be detected with ease, providing ample sensitivity for the detection of the transitions.

Also placed in the light path in the tetrahedron was a small KBr disc. The transition of the KBr from its FCC to its BCC structure at a hydrostatic pressure of 18 kbar is detected directly by observing a large discontinuity in optical transmission, and indirectly by a bismuth resistance discontinuity. This latter discontinuity is caused by the 10% volume change of the KBr, resulting in strains and permanent distortion of the surrounding bismuth layer.

The nonlinearity of the load–pressure relationship necessitates a measurement of the pressure between the fixed points obtained by the detection of the various phase transitions. This is done by studying the pressure induced shift of the absorption peak at 19 000 cm^{-1} (see Zahner and Drickamer 1960) in nickel dimethylglyoxime (Ni(DMG)$_2$), and comparing the results obtained with calibration results of Davis (1968). Some examples of room temperature calibration curves using Ni(DMG)$_2$ are given in figure 3. Curve A represents the calibration for a tetrahedron containing a large quantity of KBr, and curve B is for one containing a small quantity of KBr, the remaining voids being filled with NaCl. The two sets of data diverge above the KBr phase transition, and this is attributed to the pressure-dropping effect of the KBr volume change. The curves amply demonstrate that there is not a linear load–pressure calibration in the region of a large volume change in any high pressure apparatus which relies
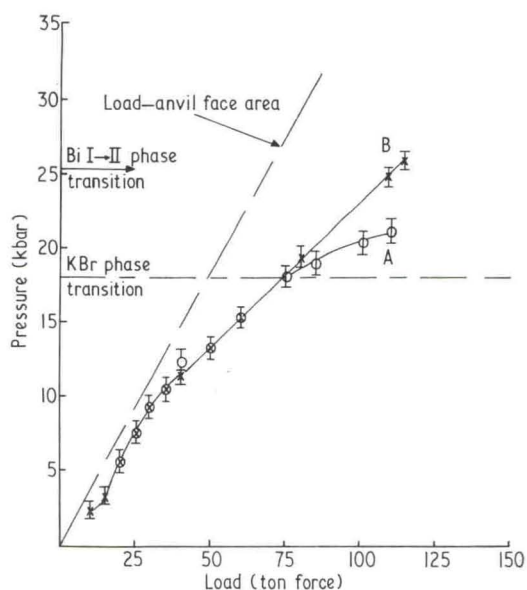
on gaskets to support the pressure. It is also seen that above and below about 10 kbar the load–pressure curve has different slopes.

4 Pressure calibration at low temperature

To obtain fixed points on the calibration curve for experiments below room temperature, the phase transitions of KBr, KCl and Bi were used. The temperature dependence of the KBr and KCl transitions have been studied down to dry ice temperature by Bridgeman (1940) and a linear extrapolation has been used in the present work for lower temperatures. The low temperature phase diagram of bismuth has been studied by several authors (Il'ina and Itskevich 1966, Roux *et al.* 1969). There is some dispute in the literature as to the existence of the transition that Il'ina and Itskevich see at low temperatures and regard as an 'electronic' rather than a crystallographic phase transition. Roux *et al.* (1969) do not see this transition.

Results during an experiment at 140 K are shown in figure 4. The experimental arrangement inside the tetrahedron was that indicated in figure 2(*b*). The region from 0 to 100 ton force is characterized by a steady decrease in optical transmission (see figure 4(*a*)), probably caused by the fracture of the clear halide discs due to distortions in the tetrahedron. This effect
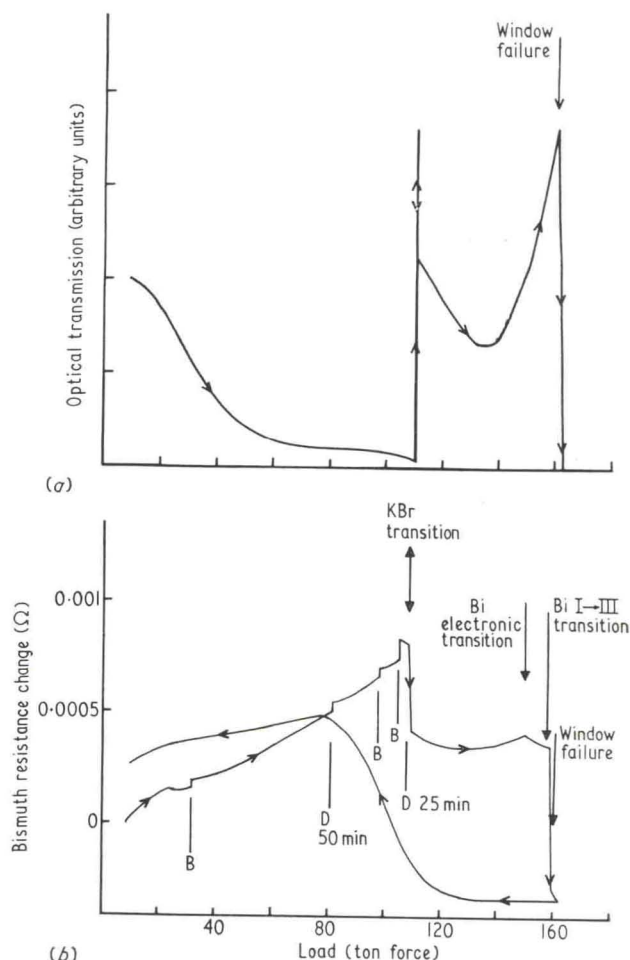
(*a*)

(*b*)

Figure 4 The upper curve shows a typical variation of optical transmission as the load is increased. The KBr phase transition and catastrophic window failure are indicated on the diagram. The lower curve shows the typical behaviour of the resistance of the bismuth, the KBr, Bi 'electronic' and Bi I → III phase changes as indicated. The results were recorded at 140 K

Figure 3 Room temperature pressure calibration curves. Curve A gives results when the tetrahedron contained a large quantity of KBr and curve B results when the tetrahedron contained a small quantity of KBr

is greater in the low load region where the gaskets undergo the largest changes.

The KBr transition at about 108 ton force is marked by a large increase in optical transmission. The applied load was kept constant at 108 ton force for 25 min. During this time the transmission increased to a maximum after 10 min, and then steadily decreased. Such an increase in transmission was not seen by Wiederhorn and Drickamer (1960) when they investigated the phase transitions in various potassium halides. Instead a sudden decrease in signal was reported. The KBr and KCl discs used in the present experiments were formed by cold compaction of the powder, whereas Wiederhorn and Drickamer used single crystal material. The discs of the present work had a slightly milky appearance caused by light scatter from voids in the polycrystalline matrix. At the phase change these voids fill and also the interfaces (such as the KBr–window interfaces) improve to give a decrease in light scattering. The multiple nucleation of the BCC high pressure phase of KBr results in grain boundary scattering and causes a decrease in transmission, but this is later followed by an increasing transmission as grain growth proceeds.

The variations with pressure of the bismuth resistance which accompany the above optical effects are shown in figure 4(b). The load was increased at intervals of 2 ton weight with pauses of duration of the order of 10 min between each increment. Over most of the range the bismuth resistance increases monotonically. At the points labelled B, discontinuous increases in resistance were recorded and were accompanied by a noise from the apparatus as gaskets adjusted to the new loading conditions. At the points labelled D, the resistance discontinuities show the changes in resistance at constant load during the periods indicated. Most of these changes occur within a few minutes, and thereafter the system remains stable. The Bi I → III transition shows clearly at 160 ton force. A change in the slope of the resistance curve is also indicated at about 152 ton force, and may be related to the 'electronic' phase transition mentioned by Il'ina and Itskevich (1966). Following a window failure at 164 ton force the load on the cell was relieved. It is found that even without window failure, the pressure calibration of the system is not the same when loading and unloading the system.

Using the tetrahedron design shown in figure 2(b) the load dependence of the absorption peak in Ni(DMG)$_2$ was measured at low temperatures. The results are shown in figure 5. The apparatus was cooled down from room temperature to 130 K at a load of 20 ton force. Then, while the
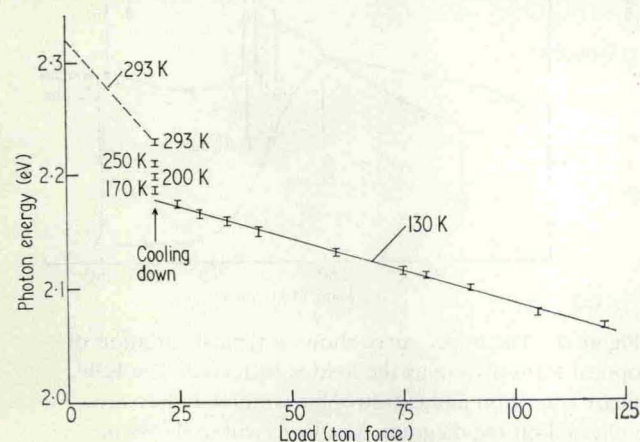
temperature was maintained constant to ± 7 K, the load was increased and the peak position monitored. It is presumed that most of the energy shift of the peak at the load of 20 ton force derives from the temperature change from 293 to 130 K rather than from changes at hydrostatic pressure due to cooling. The justification for believing this is that a similar energy shift for the band is observed at ambient pressure if the same temperature variation is applied.

The results of figure 5 show that the energy E_{130} of the absorption peak in Ni(DMG)$_2$ at 130 K is given by

$$E_{130}(p) = A + KL \tag{1}$$

where A and K are constants and L is the applied load. The KBr transition in this run occurred at 140 ton force.

If the assumption is made that the pressure shift of the Ni(DMG)$_2$ absorption peak has a similar form at low and room temperatures, then, following Davis (1968),

$$E_{130}(p) = E_{130}(p=0) + c_1 p + c_2 p^2 \tag{2}$$

where c_1 and c_2 depend upon temperature and p is the hydrostatic pressure.

Eliminating $E_{130}(p)$ from (1) and (2) gives

$$p = \{A - E_{130}(p=0)\}/c_1 + KL/c_1 \quad \text{if } c_2 \ll c_1. \tag{3}$$

At ambient pressures Davis (1968) finds $c_1 \sim 100\, c_2$.

As equation (3) represents a linear dependence of p upon L, the relationship is determined by measuring (i) the applied loads at which the Bi and KBr phase transitions occur and (ii) the energy of the Ni(DMG)$_2$ peak at the point A in figure 5, from which the hydrostatic pressure can be inferred from the room temperature calibration of Davis (1968).

5 Limitations and applications

The size of the apparatus limits its usefulness. Experiments have to be built around the press rather than vice versa. Its bulk also limits the minimum obtainable temperature and hence the diversity of permitted experiments.

The maximum obtainable pressure is limited by the breaking strain of the windows. Pressures as high as 50 kbar have been achieved. In all experiments in which the maximum pressure obtained is greater than about 5 kbar the sapphire windows are found to be cracked at the end of the experiment. The cracking is detected by a sharp reduction in the cell transmission which occurs typically at 35 ton force as the load is reduced from, say, 150 ton force (i.e. 30 kbar at 25°C). The window contains cracks throughout the entire cylinder.

At high pressures (e.g. 25 kbar) and low temperatures (e.g. 150 K) catastrophic window failure sometimes occurs, resulting in a very large reduction in transmission. The window is damaged in a different manner from that described above. The circular area near the hole in the anvil is powdered to a depth of about 1 mm. The corresponding area on the high pressure side of the window contains a triangular dimple, the apex of which is about 1 mm below the surface. The whole high pressure surface is perfectly smooth and suggests that some form of plastic deformation may have occurred. The crack density in the bulk of the window is high. Many cracks extend throughout the crystal on planes perpendicular to the cylinder axis, i.e. along the basal planes of the sapphire.

Experiments which involve the measurement of optical density are not easily carried out with the present system because of the large number of optical components in the light path. Difficulties arise on account of relative motions of one component with respect to another, resulting in changes in the overall transmission of the system. The apparatus has been used very successfully to measure the changes in energy of optical absorption lines which are clearly resolved.

Figure 5 The load dependence of the optical absorption peak in Ni(DMG)$_2$ at 130 and 293 K